978-1-5386-0774-9/17/$31.00 ©2017 IEEE 474

A concept sensor-based system to be integrated in an existing automated platform monitoring bacterial growth

Michele Bona, Michela Borghetti, Paolo Bellitti, Mauro Serpelloni, Emilio Sardini
Department of Information Engineering
University of Brescia
Brescia, Italy
m.bona002@unibs.it

***Abstract*—Bacterial infections are still one of the main causes of disease around the world. For this reason, the early diagnosis of an infection becomes fundamental for patient's health. In the market, there are very advanced systems that perform such analyses on biological samples, such as WASPLab, by COPAN Italia S.p.A. This platform monitors the growth of bacterial cultures, in a fully automated way, by taking periodic images of the Petri dishes inoculated with bacteria. In this work, we describe the preliminary study on a concept sensor-based system that, when optimized, could be integrated in the WASPLab, to provide a more rapid and complete diagnosis response. The system measures the electrical impedance related to a Petri dish instrumented with an electrode-based sensor, only at two fixed frequencies. In addition, it presents quantitative information associated to bacterial growth to the user in real time. Such information comes under the form of parameters derived from impedance response. We tested the system through a specific experimental analysis. During repeated tests, we inoculated a Petri dish with an initial concentration equal to 1.5 McFarland of *Staphylococcus Aureus* ATC 6538. We have been monitoring its growth for 18 hours, while the dish was staying in an incubator at 35°C, by measuring the impedance at 100 Hz and 1000 Hz. After six hours, we observed a variation higher than 10% on the best parameter, which allowed finding a growth detection time of four hours. Achieved results demonstrate the validity of our approach, paving the way to the possibility to integrate our device in the WASPLab, to enhance its flexibility and diagnosis capabilities.**

Keywords—bacterial growth monitoring; electrode-based sensor; impedance; Petri dish; WASPLab

I. INTRODUCTION

Bacterial infections are still one of the main causes of disease, and even of death, around the world. The situation is complicated by the fact that some bacterial species are becoming increasingly resistant to antibiotic-based therapies, as confirmed by the World Health Organization [1]. This is not true only in the developing countries. Indeed, a 2015 report from the Center for Disease Dynamics, Economics and Policy affirms that every year, in the United States, there are more than 2 million cases of bacterial infection and 23000 people die because of such phenomenon [2]. The same document talks about 25000 annual deaths in Europe [2]. For this reason, the early diagnosis of an infection becomes fundamental for patient's health. In fact, it could permit a timely action consisting in finding and delivering the right drug therapy when infection has not developed yet. A rapid intervention could save patient's life or avoid permanent damages. Consequently, an objective response about the occurrence of an infection should be achieved as early as possible.

In this scenario, an important contribution comes from systems and methods carrying out a pre-analytics action, i.e., a preliminary detection of bacterial growth in a biological sample. Such analysis allows identifying the presence of a pathogen before sending the sample to a specific laboratory for biochemical and/or serological tests, which need days to provide a more detailed answer [3].

There are numerous methods exploited for bacterial growth detection, which have been known for a long time. They rely on different physical principles. Among them, the literature cites gas chromatography [4], fluorescence spectroscopy [5], flow cytometry [6], microcalorimetry [7], surface plasmon resonance [8], and impedance microbiology [3]. Such a variety of methods allowed the increasing spread of different kinds of biosensors equipped with specific receptors for target bacteria [9]-[10].

In the same way, the market offers many commercial systems that perform pre-analytics tests on biological samples. Reference [9] reports some examples. An advanced solution comes from the WASPLab (WASP stays for Walk-Away Specimen Processor), by company COPAN Italia S.p.A [11]. This platform monitors bacterial cultures growth, in a fully automated way, by taking and analyzing periodic images of the container inoculated with bacteria. However, the possibility to add quantitative data through a measurement from a sensor to the information coming from the images would enrich the response provided by the WASPLab. This would augment its smartness and flexibility. Furthermore, since having at disposal an early objective response about infection is fundamental for

This research activity is financed through the Adaptive Manufacturing Project (CTN01_00163_216730) by the Italian "Cluster Tecnologico Nazionale Fabbrica Intelligente".

patient's health, it is desirable to obtain a signal containing enough data to anticipate image information.

For this reason, in the present work we describe the preliminary study carried out on a concept sensor-based system that, when optimized, could be integrated in the WASPLab, to provide a more complete diagnosis response and enhance its flexibility. For this purpose, we applied the principles of impedance microbiology, which associates a variation of electrical impedance to bacterial cultures growth [3]. Currently, research on this topic focuses on design and realization of technologically advanced sensors [12]-[17]. However, very few works treat the development of a complete system made by a sensor and an electronic unit elaborating its output.

The present paper is organized in the following way. The second section will talk about the existing WASPLab platform, together with the parts it is made by. The third section will illustrate our solution, describing the concept system we realized. Finally, the fourth section will present the experimental analysis we carried out to test our system and the achieved results.

II. WASPLAB PLATFORM

As already mentioned in the previous section, WASPLab is a platform that permits to monitor bacterial activity in a container, such as a Petri dish, which holds the medium necessary for cultures growth. WASPLab manages the phases of container inoculation with a pathogen, incubation, and image taking, analysis, and storing, in a fully automated way. Fig. 1 shows a representative picture of such platform. A numbered label highlights each part:

1) WASP: it is a station equipped with a robotic manipulator, which picks in sequence a Petri dish and places it where the biological sample containing the pathogen is added. For a correct operation, dishes are also opened and closed in an automatic way. A scanner recognizes every dish through a bar code. An image verification system controls the entire process;
2) Image acqusition station: it takes a High Definition image of the Petri dish at specific time instants, which are decided by platform user. A software drives image acquisition steps;
3) Incubators: there are two incubators, which create the ideal environmental conditions for bacterial growth. Temperature range is from 4°C to 40°C. Every Petri dish has its own location in the incubators, according to the corresponding bar code. Dishes are inverted to avoid that condensation falls onto the medium;
4) Dishes accumulation silos: they contain the Petri dishes that have been completely analyzed by the WASPLab. They are the places where dishes are stacked waiting for removal from the platform;
5) Digital imaging interface: it is a web-based user interface that permits to carry out the analysis on the acquired images;
6) WASPLab Central: it has a double role. On one hand, it stores all the images that are acquired and analyzed. On the other hand, it allows the WASPLab to communicate with other systems.

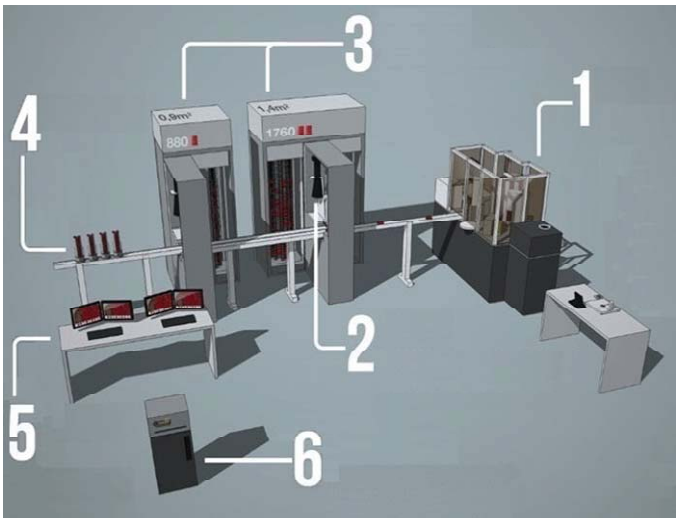

Fig. 1. The WASPLab platform.

The WASPLab works in the following way:

- a sterile Petri dish is inserted into the WASP (label 1 shown in Fig. 1), where inoculation with bacteria takes place;
- the dish is immediately transported to the image acquisition station (label 2), where its picture is taken at zero hour (i.e., the time instant of infection);
- afterwards, it is stocked in one of the two incubators (label 3), in order to foster a proper growth of bacterial colony;
- after specific intervals defined by analysis protocol, the dish is taken from the incubator and sent again to the image acquisition station, in order to obtain new pictures. Then, it is sent back to the incubator;
- platform user monitors colony growth evolution from the digital imaging interface (label 5), by analyzing the images stored in WASPLab Central (label 6);
- once the analysis is finished, the Petri dish is put in one of the accumulation silos (label 4).

III. CONCEPT SENSOR-BASED SYSTEM

We realized a system able to measure the impedance related to two Petri dishes (called A and B to distinguish them) at different frequencies. Such system is composed by three main parts. The first part is an electrode-based sensor inserted in a Petri dish like those used in the WASPLab. The second part is a portable electronic module that excites the sensor and treats the signal coming from it. The third part is a computer presenting a user interface that controls electronic module operation, elaborates the conditioned signal, and presents the information about bacterial growth in the Petri dish in real time. Fig. 2 shows system block scheme, whereas the following subsections will talk about its parts in detail.

A. Sensor embedded in the Petri dish

Fig. 3 provides a representation of the electrode-based sensor embedded in the Petri dish, through either a

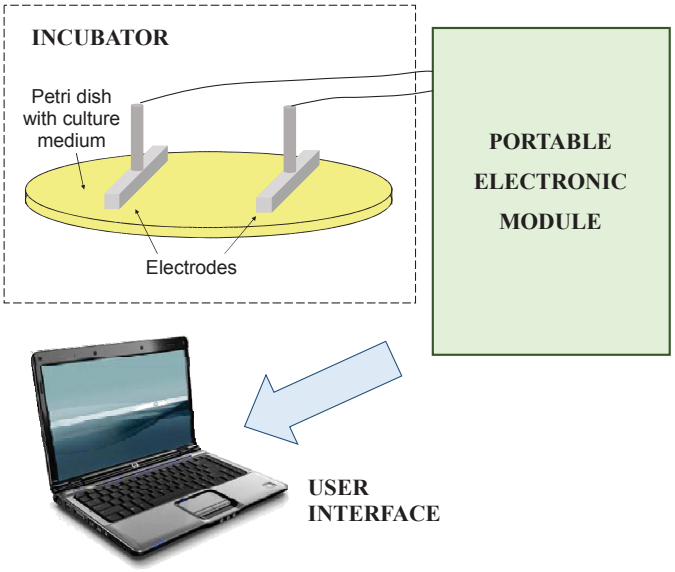

Fig. 2. Block scheme of the realized concept system.

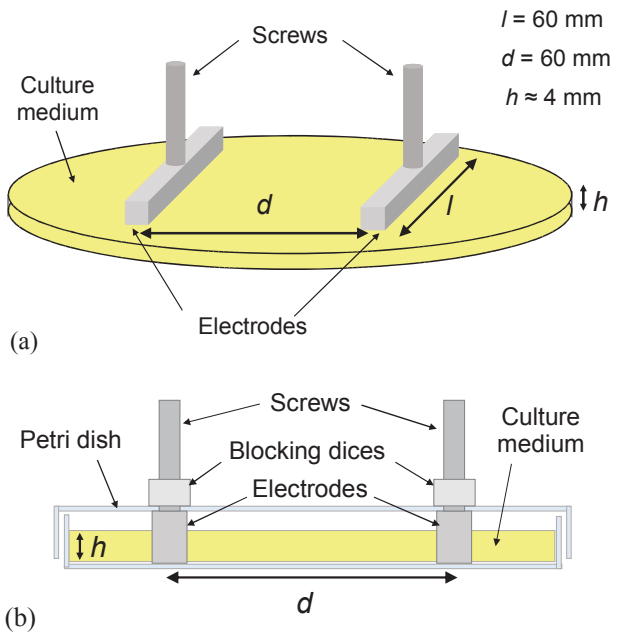

Fig. 3. Representation of the electrode-based sensor embedded in the Petri dish: (a) tridimensional view; (b) cross-section view.

tridimensional view (Fig. 3a) or a cross-section view (Fig. 3b). Since, for our concept system, we chose to implement the simplest sensor configuration as possible, we added a couple of steel electrodes with rectangular section to the Petri dish, whose diameter is equal to 85 mm. Referring to Fig. 3, electrodes have a length l equal to 60 mm and they were partially immersed in the medium for a height h of about 4 mm. They were positioned parallel to each other at a distance d equal to 60 mm. In this way, a significant portion of the culture medium contained in the Petri dish is between the electrodes, which were fixed to the dish cover through blocking dices. Finally, two steel screws protrude from the electrodes, to act as contact terminals for the measurements. After the addition of the two electrodes, the Petri dish was sterilized using gamma rays, in order to prevent any other form of contamination than the one from the pathogen being monitored.

Fig. 4a reports a qualitative graph of sensor frequency response, in terms of impedance magnitude $|Z|$ and phase angle $\angle Z$. Such behavior typically occurs when culture medium (which is an electrolyte) is interfaced to metal electrodes [3]. As can be observed, two different regions can be identified. At low frequencies (i.e., below a limit going between 1000 Hz and 10000 Hz [3]), $|Z|$ presents a decreasing trend, whereas $\angle Z$ has negative values between 0° and -90°. In this region, impedance behavior is influenced mainly by the physical phenomena occurring at the interface between electrodes and culture medium. On the other side, at higher frequencies (i.e., above the previously mentioned limit), $|Z|$ tends to assume a constant value and $\angle Z$ remains close to 0°. In this area, the impedance depends mostly on medium own characteristics.

The electrical behavior of the ensemble electrode-culture medium-electrode can be represented through a variety of equivalent models [3], [16]. They differ according to their complexity and accuracy in fitting the frequency trend shown in Fig. 4a. In this work, we chose a simple model, which is reported in Fig. 4b. It represents the interface between electrodes and medium with the parallel between capacitance C_{DL} and resistance R_{CT}. Parameter C_{DL} models the double layer

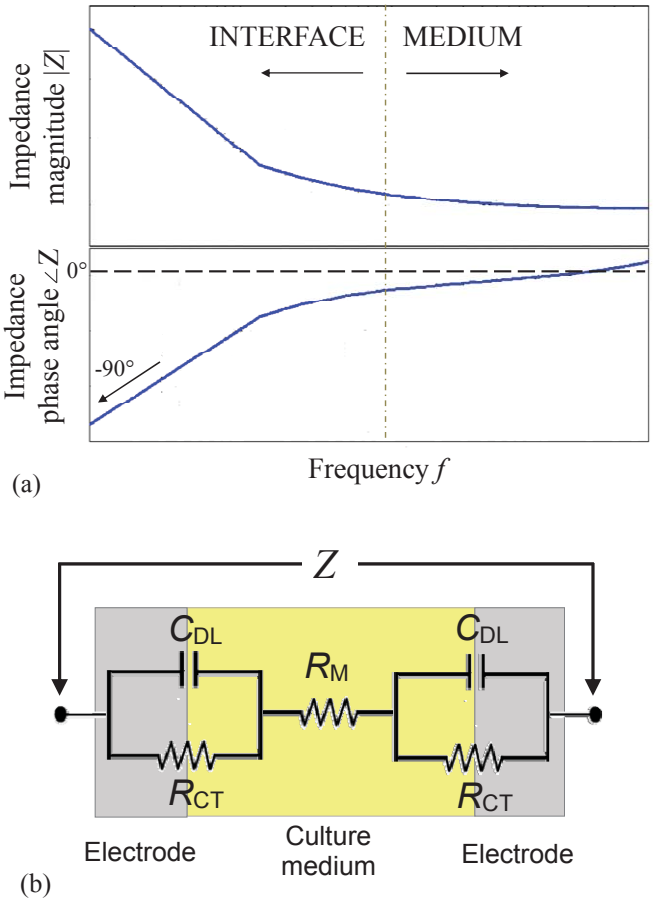

Fig. 4. (a) Qualitative graphs of the electrode-based sensor response in terms of impedance magnitude $|Z|$ and phase angle $\angle Z$ as a function of frequency f; (b) electrical equivalent model of the ensemble electrode-culture medium-electrode.

capacitance at the interface between medium and electrode. On the other hand, R_{CT} represents the charge transfer between electrode and medium. Since electrodes are identical in either geometry or fabrication material, we assumed C_{DL} and R_{CT} to have the same values for both of them. Then, the parallels between C_{DL} and R_{CT} are in series with resistance R_M, which quantifies medium conductivity.

Since the parameters of the electrical equivalent model vary in time as bacterial culture grows in the medium, their estimation provides quantitative information about growth process. As they are three, they are obtained from an impedance measurement performed only at two fixed frequencies f_1 and f_2, through the implementation of the following mathematical equations:

$$C_{DL} = \frac{f_1 / \mathrm{Im}(Z(f_1)) - f_2 / \mathrm{Im}(Z(f_2))}{\pi f_2^2 - \pi f_1^2} \tag{1}$$

$$R_{CT} = \sqrt{-\frac{\mathrm{Im}(Z(f_1))}{4\pi f_1 C_{DL} + 4\pi^2 f_1^2 C_{DL}{}^2 \mathrm{Im}(Z(f_1))}} \tag{2}$$

$$R_M = \mathrm{Re}(Z(f_2)) - \frac{2R_{CT}}{1 + 4\pi^2 f_2^2 C_{DL}^2 R_{CT}^2} \tag{3}$$

where $\mathrm{Im}(Z(f_i))$, i = 1,2, is impedance imaginary part in correspondence of f_1 or f_2, whereas $\mathrm{Re}(Z(f_2))$ is impedance real part at f_2. Therefore, measuring the impedance along the entire frequency spectrum (to obtain a graph similar to the one of Fig. 4a) is not necessary. This permits to realize and work with a system equipped with a simpler electronic unit.

B. Portable electronic module

The portable electronic module includes two distinct parts. The first one is a conditioning circuit board, whereas the second part is a data acquisition board. The electronic module is supplied by an external power source.

Conditioning board was fabricated through printed circuit board techniques using discrete components. Fig. 5 shows its schematic diagram. It presents a Direct Digital Synthesizer (DDS) that generates three kinds of sinusoidal voltage signal. The first one (V_{PA}) is the in-phase signal exciting the sensor inserted in Petri dish A. The second one (V_{PB}) is the in-phase wave that excites the sensor of dish B. Finally, the third one (V_Q) is the quadrature signal related to each in-phase wave. Excitations occur at different times. In fact, one measurement cycle consists of five phases. During the first phase (*ph*1), the DDS excites the sensor embedded in Petri dish A at frequency f_1. In the second phase (*ph*2), it provides the excitation signal to the sensor inserted in dish B at f_1. Then, during the third and fourth phases (*ph*3 and *ph*4), it excites the sensors of dish A and dish B, respectively, but at frequency f_2. Finally, in the fifth phase (*ph5*), the DDS generates a DC signal. Therefore, according to cycle phase, only one sensor is excited at a time, and the relative quadrature signal is generated. In addition, the signals are shifted in order to eliminate the DC component. In this way, V_{PA}, V_{PB}, and V_Q have the following expressions in each phase:

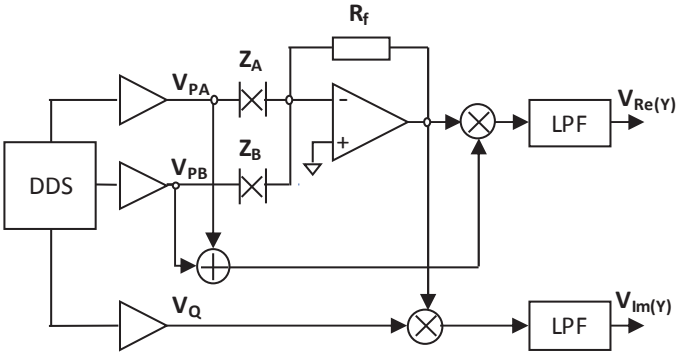

Fig. 5. Schematic diagram of the conditioning circuit board.

$$V_{PA} = \begin{cases} \sin(2\pi f_1 t) & ph1 \\ \sin(2\pi f_2 t) & ph3 \\ 0 & ph\{2,4,5\} \end{cases} \tag{4}$$

$$V_{PB} = \begin{cases} \sin(2\pi f_1 t) & ph2 \\ \sin(2\pi f_2 t) & ph4 \\ 0 & ph\{1,3,5\} \end{cases} \tag{5}$$

$$V_Q = \begin{cases} \cos(2\pi f_1 t) & ph\{1,2\} \\ \cos(2\pi f_2 t) & ph\{3,4\} \\ 0 & ph5 \end{cases} \tag{6}$$

The first four phases have a duration equal to 10 seconds, whereas the fifth phase lasts until measurement cycle ends. The terminals of each electrode-based sensor are inserted between the shifter and the negative input of a dedicated inverting amplifier. Amplifier output is multiplied by the excitation signal and low-pass filtered to isolate DC component ($V_{Re(Y)}$). This is a voltage signal proportional to the real part of the admittance related to each Petri dish measured at the selected frequency. Furthermore, the same amplifier output is multiplied by the quadrature signal and low-pass filtered to isolate the respective DC component ($V_{Im(Y)}$), which is proportional to the imaginary part of dish admittance. Full scale measurement range is between -5 V and 5 V.

Signals $V_{Re(Y)}$ and $V_{Im(Y)}$ are the outputs of the conditioning circuit board. They are then collected by data acquisition board, which includes 12-bit analog-to-digital converters, in order to be elaborated.

C. User interface

User interface is implemented through a custom LabVIEW Virtual Instrument (VI), which runs on a personal computer. Such VI performs different tasks. First, it manages measurement timing, by sending specific commands to the DDS via Serial Peripheral Interface, for properly exciting the two electrode-based sensors according to the occurring cycle phase. Second, it acquires the outputs of the conditioning circuit board, which have been previously converted by the data acquisition board, to elaborate them. Such elaboration takes place through two steps. Initially, converted outputs are transformed into impedance values. In particular, impedance

real part Re(Z) and imaginary part Im(Z) at both frequencies f_1 and f_2 are obtained. Then, (1), (2), and (3) are implemented to calculate parameters C_{DL}, R_{CT}, and R_M from Re(Z) and Im(Z). Third, the VI presents data about either impedance values or calculated equivalent parameters to system user, through both graphical tools and numerical indicators, in real time. In this way, user can monitor their trend at any time of measurement process. Fourth, it saves all these data in a *.txt* file, at the end of each measurement cycle. Therefore, they are always available for further offline elaboration and visualization through common software platforms, such as Microsoft Office and Mathworks MATLAB. Last, it permits to set various measurement process parameters, such as f_1, f_2, and cycle duration. These frequencies can be selected among a range going from few hertz to some kilohertz, which depends on conditioning board characteristics. Cycle duration should last about one minute at least, taking into account the duration of all the phases. In addition, user can select if performing single or continuous measurements. In the second case, system works in a fully automatic way, and no further operations are requested to the user until the end of the measurement session. These possibilities of choice give a great level of flexibility to the system, which can adapt to operate at different conditions, according to the application and to user necessity.

IV. Preliminary Experimental Analysis

We tested the device through a specific experimental analysis. We carried out repeated tests, following always the same protocol.

A. Followed experimental protocol

Two instrumented Petri dishes were filled with a culture medium based on Tryptone Soya Agar, which contains all the nutrients necessary to a bacterial colony to grow. Afterwards, one of them was inoculated with a solution presenting an initial concentration equal to 1.5 McFarland (equivalent to $4.5 \cdot 10^8$ CFU/ml) of pathogen *Staphylococcus Aureus* ATC 6538. In particular, all the area between the electrodes was occupied, in order to achieve an impedance variation associated with bacterial growth as great as possible and, therefore, the maximum measurement sensitivity. Such procedure was carried out at ambient temperature. On the contrary, the other Petri dish was kept sterile. In this way, we had a reference for a comparison with the behavior characterizing the infected plate.

Just after inoculation step, we put both dishes in an incubator, which recreated the ideal growth conditions reached when using the WASPLab. Incubator internal temperature was set to a constant value equal to 35 °C. We turned on the incubator about one hour before putting the dishes in it, in order to guarantee a uniform internal temperature.

Once the setup was ready, test could start. Our system performed the desired measurement on the Petri dishes at the two frequencies of interest. We chose f_1 = 100 Hz and f_2 = 1000 Hz, as such frequencies are both in the region when impedance variation is significant (see Section III.A). We have been monitoring the changes in the impedance and in parameters C_{DL}, R_{CT}, and R_M linked to bacterial growth for 18 hours from inoculation time. We set conditioning board cycle to perform a measurement every two minutes.

B. Achieved results and discussion

Fig. 6 provides a picture of the infected Petri dish taken at the end of one of the performed tests. It should be noted how bacterial growth generated a film that changed medium color. Consequently, this image permits to distinguish the inoculated area (which is highlighted) from the rest of the surface.

Fig. 7 shows the time evolution of impedance at f_1 and f_2, which is associated to the Petri dish shown in Fig. 6 and the corresponding sterile one. In particular, impedance is represented as relative magnitude $|Z|^*$ and relative phase angle $\angle Z^*$ with respect to their initial values. They are defined as:

$$|Z|^* = \frac{|Z|}{|Z|_{t=0}} \tag{7}$$

$$\angle Z^* = \angle Z - \angle Z_{t=0} \tag{8}$$

where $|Z|_{t=0}$ and $\angle Z_{t=0}$ are the first magnitude and phase angle values obtained during the test, respectively. In this way, the impedance behaviors characterizing the two Petri dishes can be compared regardless of the differences in their absolute values. We obtained $|Z|$ and $\angle Z$ from Re(Z) and Im(Z) (which are provided by the system) through the implementation of trigonometric formulas.

Fig. 7a highlights that all $|Z|^*$ curves present an initial transient lasting about one hour. This is probably due to medium temperature settling from ambient temperature to 35 °C, with consequent partial drying. However, after about five hours, $|Z|^*$ curves related to the infected Petri dish begin to assume a different trend, which is caused by bacterial growth. On the other side, Fig. 7b permits to draw similar conclusions. In fact, $\angle Z^*$ curves associated with sterile dish

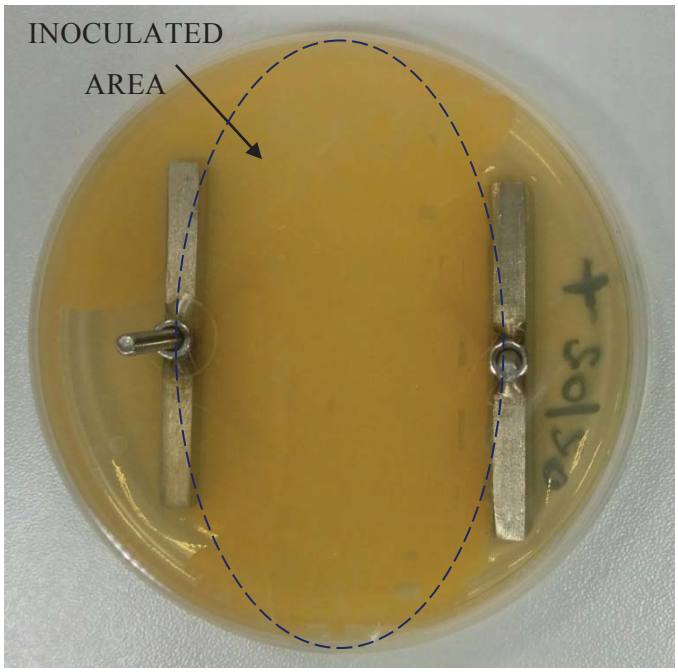

Fig. 6. Picture of the infected Petri dish taken at the end of one of the performed tests. Inoculated area is highlighted.

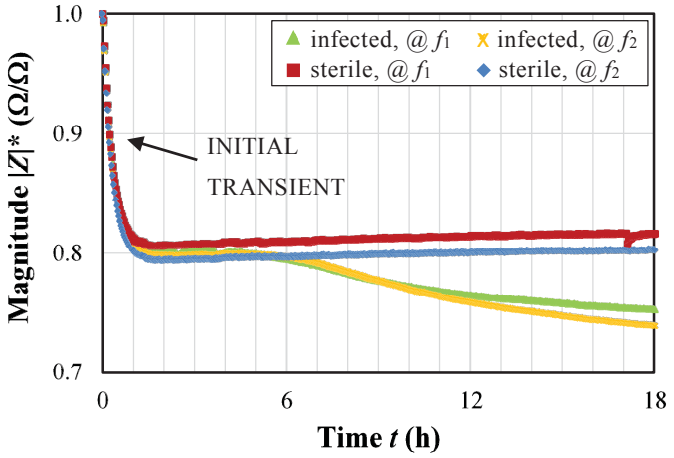

(a)

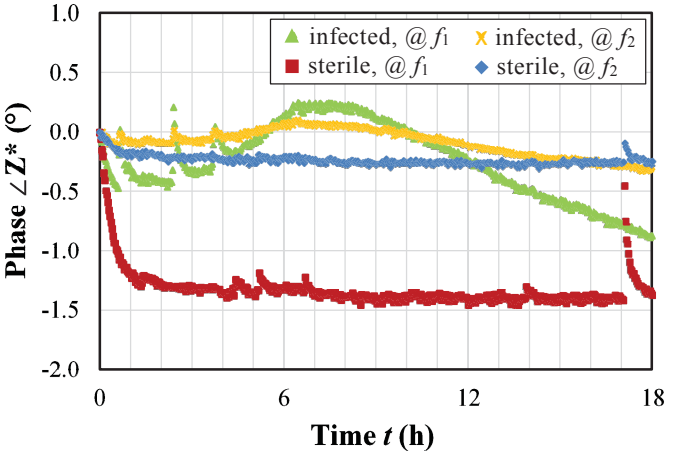

(b)

Fig. 7. Impedance at f_1 and f_2 as a function of time, for the infected Petri dish shown in Fig. 6 and the corresponding sterile one: (a) relative magnitude $|Z|$*; (b) relative phase angle $\angle Z$*.

are almost stable after the initial transient, whereas those related to the infected plate present additional variations depending on pathogens activity.

Fig. 8 reports the values assumed over time by the parameters of the equivalent model of the ensemble electrode-culture medium-electrode, for both inoculated and sterile Petri dishes, corresponding to the impedance values reported in Fig. 7. As for the graphs of Fig. 7, all the curves present in Fig. 8 have an initial transient of about one hour, depending probably on medium temperature settling. In addition, those related to the sterile plate have only a slight variation after the first hour, which may be due to medium drying. On the contrary, the trends characterizing the parameters associated to the infected dish reflect a typical bacterial growth curve [3], even though with different timing. In particular, if the initial transient is left out, a clear change in curves slope can be appreciated. This occurs after the fourth hour in Fig. 8a and Fig. 8b, when C_{DL} starts to increase more quickly and R_{CT} begins to decrease more rapidly, respectively. On the other hand, slope variation happens between sixth and seventh hour in Fig. 8c, when R_M starts to decrease after a constant phase. These changes can be ascribed to bacterial growth, since they are not noticed in the

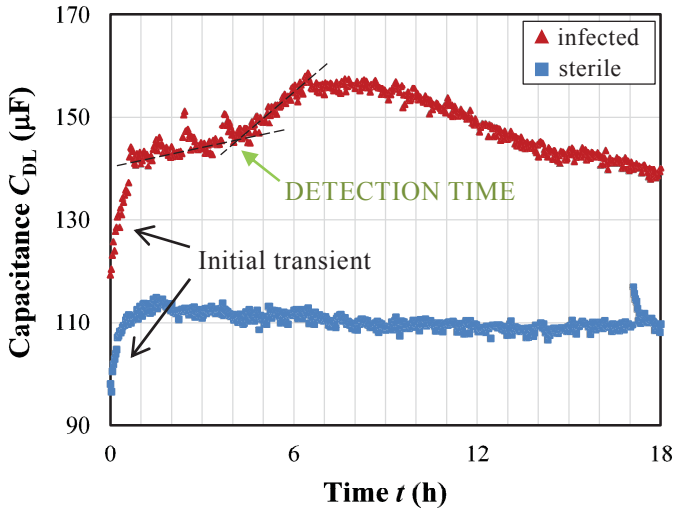

(a)

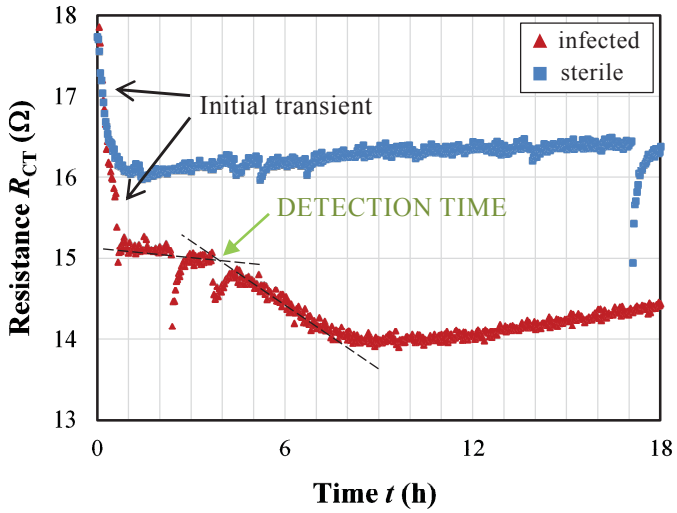

(b)

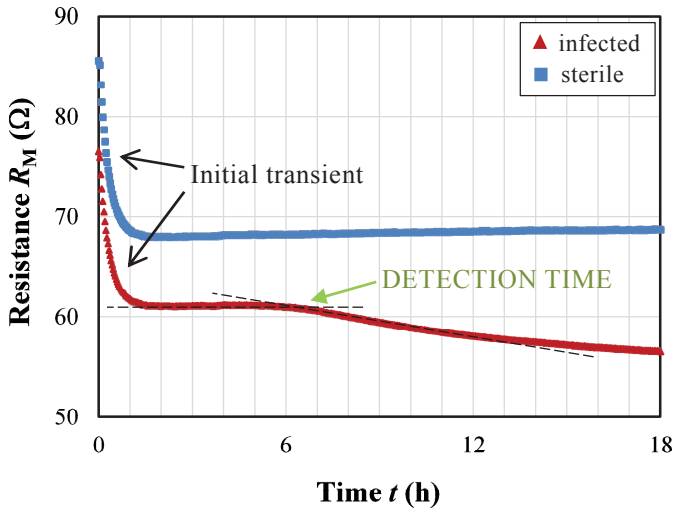

(c)

Fig. 8. Parameters of the equivalent model of the ensemble electrode-culture medium-electrode as a function of time, corresponding to the impedance values reported in Fig. 7: (a) capacitance C_{DL}; (b) resistance R_{CT}; (c) resistance R_M.

TABLE I. VALUES OF THE EQUIVALENT PARAMETERS AFTER EACH HOUR AND THEIR VARIATION WITH RESPECT TO THE VALUES AT t = 1 h

Time (h)	Capacitance C_{DL}			Resistance R_{CT}			Resistance R_M		
	Value (μF)	*Variation* (μF)	*%Variation*	*Value* (Ω)	*Variation* (Ω)	*%Variation*	*Value* (Ω)	*Variation* (Ω)	*%Variation*
0	119.406	/	/	18.212	/	/	76.553	/	/
1	140.899	/	/	15.058	/	/	61.836	/	/
2	144.277	3.378	2.398	15.151	0.094	0.621	61.057	-0.779	-1.260
3	144.307	3.408	2.419	14.955	-0.103	-0.682	61.103	-0.733	-1.185
4	146.990	6.091	4.323	14.682	-0.376	-2.495	61.165	-0.670	-1.084
5	149.014	8.115	5.760	14.718	-0.340	-2.256	61.153	-0.683	-1.104
6	155.586	14.688	10.424	14.466	-0.591	-3.927	60.968	-0.867	-1.403
7	154.391	13.492	9.576	14.133	-0.925	-6.144	60.656	-1.180	-1.908
8	155.559	14.660	10.405	13.992	-1.066	-7.076	60.056	-1.780	-2.878
9	154.472	13.574	9.634	13.982	-1.076	-7.146	59.448	-2.388	-3.862
10	154.371	13.473	9.562	14.004	-1.053	-6.996	58.913	-2.923	-4.726
11	152.797	11.899	8.445	14.059	-0.998	-6.630	58.444	-3.392	-5.485
12	148.583	7.685	5.454	14.063	-0.995	-6.609	58.053	-3.783	-6.117
13	145.750	4.852	3.443	14.129	-0.929	-6.170	57.737	-4.099	-6.628
14	142.358	1.460	1.036	14.120	-0.937	-6.224	57.481	-4.354	-7.041
15	143.759	2.860	2.030	14.249	-0.808	-5.368	57.174	-4.662	-7.539
16	142.616	1.718	1.219	14.369	-0.689	-4.574	56.919	-4.917	-7.951
17	140.368	-0.531	-0.377	14.365	-0.693	-4.601	56.731	-5.104	-8.254
18	140.153	-0.746	-0.529	14.437	-0.621	-4.121	56.539	-5.297	-8.566

curves related to the sterile dishes. Their identification occurs at the time instant at which realized system is able to detect pathogens activity (detection time). Therefore, from Fig. 8a and Fig. 8b, it can be seen how our concept system analyzing C_{DL} and R_{CT} trends has a detection time equal to four hours. However, Fig. 8c highlights that, in case of R_M monitoring, detection time moves between six and seven hours.

Additional quantitative information comes from Table I, which gathers the absolute values assumed by C_{DL}, R_{CT}, and R_M at the end of every hour of the test. Furthermore, it includes their absolute and percentage variations with respect to the values after one hour, i.e., at the end of the initial transient. Table I helps identifying the sudden increase in parameters variation in correspondence of detection time. Indeed, C_{DL} percentage variation passes from 2.419% at the end of the third hour to 4.323% after four hours, whereas R_{CT} change goes from -0.682% to -2.495% at the same time. On the other side, R_M percentage variation passes from -1.104% after five hours to -1.403% at the end of the sixth hour (variation rate further increases in the following hours). Therefore, user can set a quantitative threshold (e.g., 4% for C_{DL}) beyond which system reports automatically that bacterial growth has occurred.

In addition, Table I provides data about the extent of parameters variation during bacterial growth and, therefore, about system sensitivity to detect pathogens activity. Maximum increase in C_{DL} is greater than 10%, which occurs at the end of the sixth hour. On the other hand, R_{CT} reaches a maximum decrease higher than 7%, after the ninth hour. On the contrary, the greatest variation in R_M is achieved only at the end of the test, and it is bigger than 8%.

We reported the results obtained from one of the performed tests, since those achieved from the others are analogous, especially considering the observed trends. Indeed, the main differences concern the absolute values of both impedance and electrical equivalent parameters. Such discrepancies are likely due to the quantity of medium contained in a Petri dish, which is not the same for all the dishes.

Obtained results suggest that bacterial growth affects the behavior at the interface between electrodes and culture medium more than the characteristics of the medium itself. In particular, for our system, C_{DL} is the parameter that offers the best response, in terms of either promptness and variation extent. However, since realized system monitors either the behavior at the interface or medium conductivity, a change of R_M can represent a confirmation of what has been already disclosed through C_{DL} and R_{CT} variation. This permits to augment system reliability.

Anyway, realized system is able to automatically perform a measurement at any instant of bacterial growth process. Therefore, it could provide useful quantitative data to identify different growth phases. These data could integrate the information acquired through the image analysis performed by

the WASPLab, thus enhancing its diagnosis capabilities. In addition, a richer information could augment WASPLab smartness and flexibility. All the data could be stored in WASPLab Central, made available to other platforms through the cloud station, or processed through Big Data analytics software. In addition, having at disposal an electrical signal able to anticipate image response could favorite infection early diagnosis, which is fundamental for patient's health. For instance, Petri dishes without infection can be discarded before taking successive images. In this way, report management can be faster and new dishes can be inserted in WASPLab's incubators more rapidly. Furthermore, if required, the system can be utilized to perform a pre-analytics action when dishes are directly inside the incubators. Therefore, there would not be the necessity to pick them and to send them to the image acquisition station, avoiding to introduce perturbations on growth conditions.

V. Conclusions

In this paper, we have presented the preliminary study carried out on a concept sensor-based system that exploits the principles of impedance microbiology to continuously monitor bacterial cultures growth in a Petri dish. The study aimed at investigating the possibility to integrate such a system in the WASPLab automated platform, commercialized by COPAN Italia S.p.A. Realized system measures the impedance related to a Petri dish instrumented with an electrode-based sensor, only at two fixed frequencies. Then, it presents quantitative information associated to bacterial growth to the user in real time. The parts composing our concept system have been described. Furthermore, we have presented the experimental analysis performed to test it. The followed experimental protocol has been illustrated and the achieved results have been reported. In particular, data about system detection time and sensitivity to bacterial activity have been highlighted.

Obtained results demonstrate the validity of our approach, paving the way to the possibility of integrating our system in the WASPLab. In fact, realized system is able to automatically perform a measurement (either single or continuous) during any instant of bacterial growth process. Therefore, it could offer useful quantitative data (in terms of both timing and impedance values) that could complete the information coming from the image analysis performed by the WASPLab.

For this reason, the next step is going to be the optimization of our concept system to permit its integration directly in the WASPLab. For instance, now the system can operate only with two Petri dishes. Therefore, we are going to work in the direction of allowing a more powerful and flexible interaction between electronic unit and instrumented dishes. In this way, the former could manage the measurement information coming from a greater number of plates. In addition, we are going to design and fabricate more technologically advanced electrodes, in order to augment device sensitivity to bacterial growth.

Acknowledgment

The authors would like to thank Roberto Paroni, Stefania Fontana, and Giorgio Triva, from COPAN Italia S.p.A., for the useful information about WASPLab operation and their support in the execution of the experimental tests.

References

[1] "Antimicrobial resistance: global report on surveillance," WHO Library Cataloguing-in-Publication Data, ISBN 978 92 4 156474 8, France, 2014.

[2] Center for Disease Dynamics, Economics & Policy, "State of the world's antibiotics," CDDEP, Washington, D.C., 2015.

[3] L. Yang and R. Bashir, "Electrical/electrochemical impedance for rapid detection of foodborne pathogenic bacteria," Biotechnol. Adv., vol. 26, pp. 135-150, 2008.

[4] Y. Henis, J.R. Gould, and M. Alexander, "Detection and identification of bacteria by gas chromatography," Appl. Microbiol., vol. 14, no. 4, pp. 513-524, Jul. 1966.

[5] H.E. Giana, L. Silveira Jr., R.A., Zângaro, M.T.T. Pacheco, "Rapid identification of bacterial species by fluorescence spectroscopy and classification through principal components analysis," J. Fluoresc., vol. 13, no. 6, pp. 489-493, Nov. 2003.

[6] I.O.L. McHugh and A.L. Tucker, "Flow cytometry for the rapid detection of bacteria in cell culture production medium," Cytometry A, vol. 71, no. 12, pp. 1019-1026, Dec. 2007.

[7] O. Braissant et al., "Isothermal microcalorimetry accurately detects bacteria, tumorous microtissues, and parasitic worms in a label-free well-plate assay," Biotechnol. J., vol. 10, pp. 460-468, 2015.

[8] H. Baccar et al., "Surface plasmon resonance immunosensor for bacteria detection," Talanta, vol. 82, pp. 810-814, 2010.

[9] D. Ivnitski, I. Abdel-Hamid, P. Atanasov, and E. Wilkins, "Biosensors for detection of pathogenic bacteria," Biosens. Bioelectron., vol. 14, pp. 599-624, 1999.

[10] K. Warriner and A. Namvar, "Biosensors for Foodborne Pathogen Detection. Agricultural and Related Biotechnologies," in Comprehensive Biotechnology, 2nd ed., vol. 4, 2011, pp. 659-674.

[11] http://products.copangroup.com/index.php/products/lab-automation/wasplab

[12] J. Paredes, S. Becerro, and S. Arana, "Label-free interdigitated microelectrode based biosensors for bacterial biofilm growth monitoring using Petri dishes," J. Microbiol. Methods, vol. 100, pp. 77-83, 2014.

[13] N. Couniot, D. Flandre, L.A. Francis, and A. Azfalian, "Signal-to-noise ratio optimization for detecting bacteria with interdigitated microelectrodes," Sens. Actuators B Chem., vol. 189, pp. 43-51, 2013.

[14] X. Tang et al., "A new interdigitated array microelectrode-oxide-silicon sensor with label-free, high sensitivity and specificity for fast bacteria detection," Sens. Actuators B Chem., vol. 156, pp. 578-587, 2011.

[15] R.D. Das, A. Dey, S. Das, and C. RoyChaudhuri, "Interdigitated electrode-less high-performance macroporous silicon structure as impedance biosensor for bacteria detection," IEEE Sens. J., vol. 11, no. 5, pp. 1242-1252, May 2011.

[16] M. Varshney and Y. Li, "Interdigitated array microelectrodes based impedance biosensors for detection of bacterial cells," Biosens. Bioelectron., vol. 24, pp. 2951-2960, 2009.

[17] M.S. Webster, I.V. Timoshkin, S.J. Macgregor, and M. Mattey, "Computer aided modelling of an interdigitated microelectrode array impedance biosensor for the detection of bacteria," IEEE Trans. Dielectr. Electr. Insul., vol. 16, no. 5, pp. 1356-1363, Oct. 2009.